INDIAN SPACE RESEARCH ORGANISATION

nrsc

Indian Ocean Surface Currents Using OSCAT and Saral-AltiKa

Version 1.0

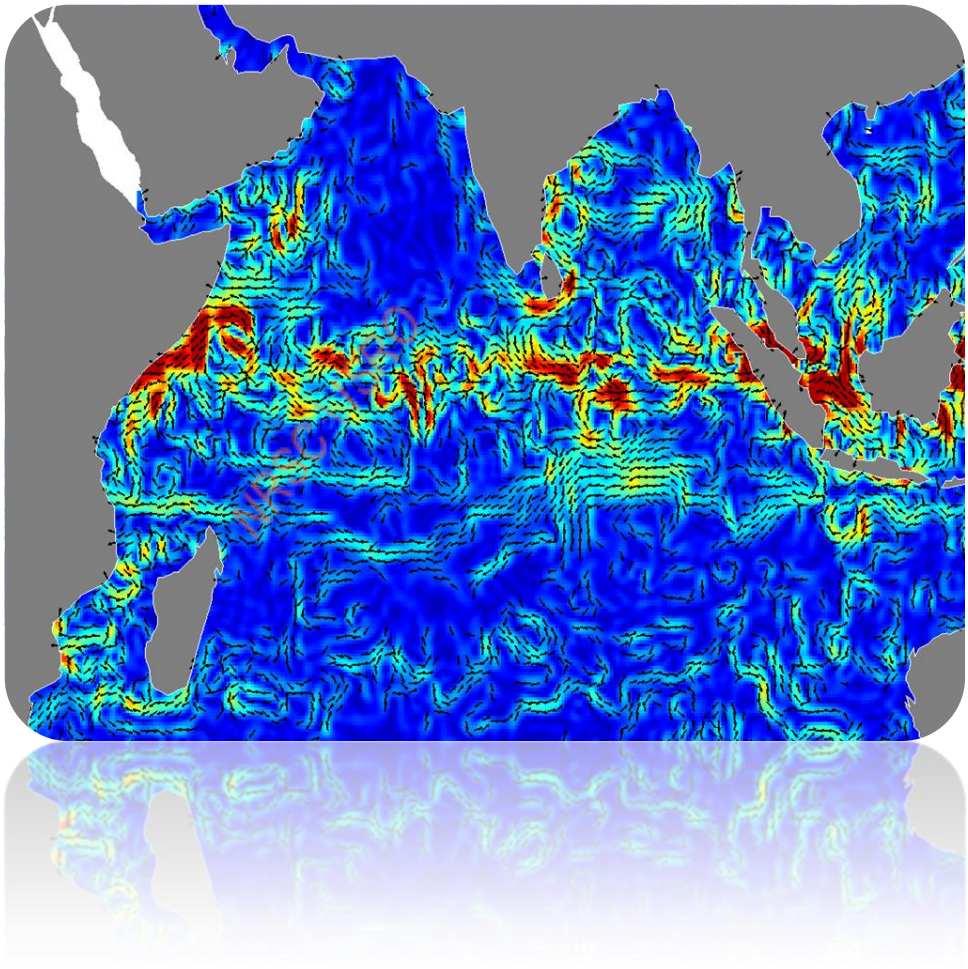

Ocean Sciences Group
Earth and Climate Science Area
NATIONAL REMOTE SENSING CENTRE
Hyderabad, INDIA

November, 2014

NATIONAL REMOTE SENSING CENTRE
REPORT / DOCUMENT CONTROL SHEET

1.	**Security Classification**	Unclassified		
2.	**Distribution**	Through soft and hard copies		
3.	**Report / Document version**	**(a) Issue no.:**01	**(b) Revision: 01** **Date:** November, 2014	
4.	**Report / Document Type**	Technical Report		
5.	**Document Control Number**	NRSC-ECSA-OSG-NOV-2014-TR-659		
6.	**Title**	Indian Ocean surface currents using OSCAT and Saral-AltiKa.		
7.	**Particulars of collation**	**Pages:** 21	**Figures:** 12 **Tables:** 5	**References:** 20
8.	**Author (s)**	Saurabh Bansal, S.K. Sasamal, K. H. Rao and C. B. S. Dutt		
9.	**Affiliation of authors**	Ocean Sciences Group, ECSA, NRSC, Hyderabad;		
10.	**Scrutiny mechanism**	**Compiled by** Saurabh Bansal, OSG (ECSA)	**Reviewed by** GD (OSG)	**Approved by** DD (ECSA)
11.	**Originating unit**	Ocean Sciences Group, ECSA, NRSC		
12.	**Sponsor (s) / Name and Address**	NRSC, Balanagar, Hyderabad		
13.	**Date of Initiation**	April, 2014		
14.	**Date of Publication**	November, 2014		
15.	**Disclaimer**	Products need to be utilized under expert supervision and due permission from the authors.		
16.	**Abstract:** The ocean surface currents are estimated from satellite observations of surface wind from Oceansat-2 Scatterometer and Sea Surface height from SARAL AltiKa. The Ekman Surface current estimated from wind stress components and geostrophic current estimated form SARAL AltiKa are combined to generated ocean surface currents. The data sets available since March 2013. The products are validated with drifting buoy observations indicating a good relationship between the observations. **Keywords:** Ocean surface current, Ekman surface current, Geostrophic current Indian Ocean			

Contents

Executive Summary

The ocean surface currents of the north Indian Ocean are estimated combining Ekman Surface Current (ESC) and Surface Geostrophic Current (SGC). The ESC is derived from the ocean surface wind fields of Oceansat-2 Scatterometer (OSCAT) data products. The path wise observations of OSCAT wind vector are used after removing high frequency variations with Data Interpolating Variational Analysis (DIVA). These winds are converted to wind stress components of zonal and meridional direction. These components used in the estimation of Ekman surface current adopting well established methods proposed by Lagerloef et al. (1999). Similarly, the SGC component of the current is estimated using SARAL AltiKa Sea Surface Height (SSH) products. Towards the geostrophic current, along track data are interpolated to quarter degree maps on daily basis. The gridded maps are used in the estimation of SGC of the Indian Ocean with reference to local Coriolis force. The Coriolis force amplifies its influence in the equatorial region within 5 degree on either side of the equator, a double differential method of surface slope is adopted to estimate the SGC. Further, the combination of SGC and ESC lead to Ocean Surface Current. The estimations at present are restricted to the north Indian Ocean.The comparison made with moored current meter observations along the Indian coast in the Bay of Bengal has shown a positive relationship with R values in the range of 0.55 to 0.64 and a negative bias of 2 to 3 cm/s in their zonal and meridional components. The products are planned to be distributed through NICES portal of Bhuvan/NRSC web site. The scope of the current observations can be seen in the navigation and optimization of shipping routes, dispersion and drift of pollutants, particularly, algal blooms and oil spills, besides their use in tracing mass and heat distribution across the ocean boundaries.

List of Figures

Figure **Page Number**

List of Tables

Table **Page Number**

1. Introduction

Traditional methods of ocean current estimation and analysis are being replaced by drifting buoys and periodic observations with advanced instruments. Recent advances in space based scatterometer and altimeter data acquisition and analysis has started providing ocean currents at regular intervals. The regular estimates of ocean currents are of vital importance to many oceanographic applications like ship routing, oil-spills advection estimation, climatic studies etc. Indian Space Research Organisation (ISRO) has launched Oceansat-2 Scatterometer (henceforth OSCAT) and recently SARAL-AltiKa altimeter that provide data products which support improvements in the estimation of ocean currents. The products from both these satellites have been used to generate products related to ocean surface currents at the spatial resolution of 0.25° x 0.25° on daily basis. These products are expected to be utilized in the studies of dispersion analysis of marine pollutants like algal blooms, coastal sediments, oil spills and debris.

This work estimates ocean surface current for the Indian Ocean. These currents have significant contribution in driving the Asian Monsoon. The currents are known for its reversal with the change of monsoon wind, one of major driving forces for the movement of the ocean waters in the surface layer. Being a land-locked area, unlike the Pacific and the Atlantic Ocean, the topography introduces diversities into the ocean currents. This leads to a change in convergence and divergence zones linking frontal boundaries and upwelling areas. In turn the currents influence the local productivity, thus the biological resources mostly marine fisheries, one of the major livelihoods for the coastal population. Further the change in heat and mass transport in the area drives the monsoon rainfall over the Indian sub-continent. This also changes the cyclone development areas at the sea and their path and intensity. Besides the changes observed in heat and mass, surface current also influence the local biodiversity, observed around the islands and coastal waters of the area. Hence the data finds a good scope of its utility in the study of ocean processes.

The ocean currents studied earlier with hydrographic observations, current meters and drifting buoys were limited to selected waters and specific periods of time. Recent observations with satellite based studies are providing opportunities to improve over the traditional knowledge, thus resolving the mysteries of migration of biological resources to the business and the economics of the coastal states. This work follows the methods adopted for real time ocean surface current analysis by Lagerloef et al. (1999). The work however uses the ocean wind and sea surface height data of the OSCAT and the SARAL products as primary inputs to estimate ocean surface currents in the Indian region.

The document provides details on estimation of Ekman Currents, Sea Surface Height, Geostrophic Currents and Total Currents using OSCAT and AltiKa data. OSCAT and AltiKa

(only for Indian Users) data products can be acquired from the web sites of the SAC-MOSDAC (Ahmadabad) and NRSC (Hyderabad). The AltiKa data is also available on AVISO ftp server for global users. The description of the products used for the estimation of ocean surface currents is provided in section 2. The results along with methodology and validation are discussed in later sections. The document also provides products description and file details with naming convention and format.

2. Data and Methods

Two primarily components of the ocean surface current are namely, the wind-driven currents and the geostrophic currents (Stommel, 1960; Price et al., 1987; Sundre and Morrow, 2008). The wind-driven currents have been derived using the OSCAT wind data following the method developed by Ekman and adopted by Bonjean and Lagerloef (2002). While the geostrophic currents is derived using Saral-AltiKa sea surface height estimations. A brief description of the two satellites has been provided below.

2.1 OSCAT Products

Oceansat-2 was launched by PSLV-C14 from Satish Dhawan Space Centre, Sriharikota on Sept. 23, 2009. It carries three payloads of Scatterometer (OSCAT), Ocean Colour Monitor (OCM) and Radio Occultation Sounder for Atmospheric Studies (ROSA).

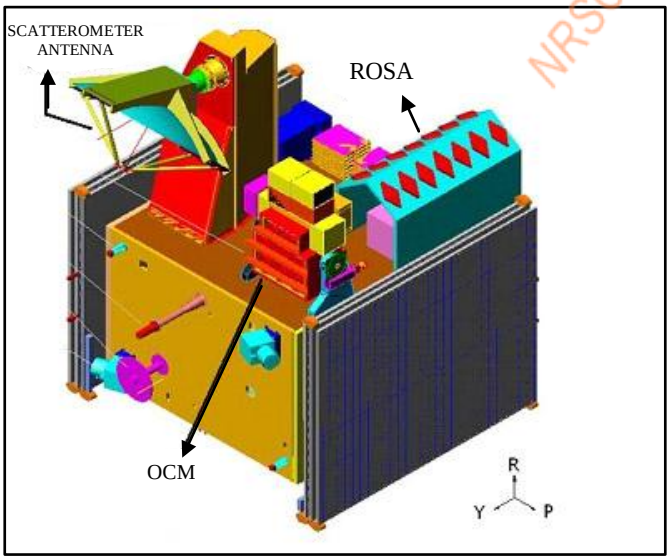

Operator	Indian Space Research Organisation
Bus	IRS
Mission type	Oceanography
Launch date	23 September 2009
Carrier rocket	PSLV-C14
Launch site	Satish Dhawan Space Centre
COSPAR ID	OCEANS2
Mass	960 kilograms (2,100 lb)
Orbital elements	
Regime	Sun-Synchronous Circular orbit
Inclination	98.280°
Apoapsis	720 kilometres (450 mi)
Periapsis	720 kilometres (450 mi)
Orbital period	99.31 minutes

Figure 1: OceanSat-2 satellite and launch characteristics.

OSCAT, ku-band (13.515 GHz) scatterometer, is a conically scanning pencil beam scatterometer which is designed and developed at ISRO/SAC, Ahmedabad. OSCAT covers a continuous swath of 1400 km for inner beam and 1840 km outer beam respectively, and provides a ground resolution of 50 × 50 km. The system works with a 1-m parabolic dish antenna and a dual feed assembly to generate two pencil beams and is scanned at a rate of

20.5 rpm to cover the entire swath. The aim is to provide global ocean coverage and wind vector retrieval with a revisit time of 2 days.

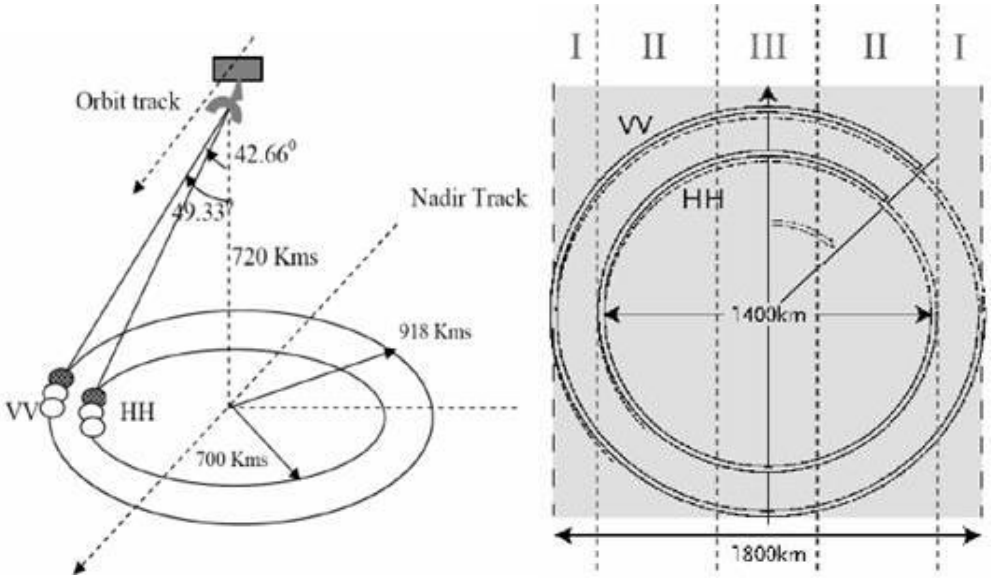

Figure 2: OSCAT – A rotating pencil beam scatterometer with details of swath.

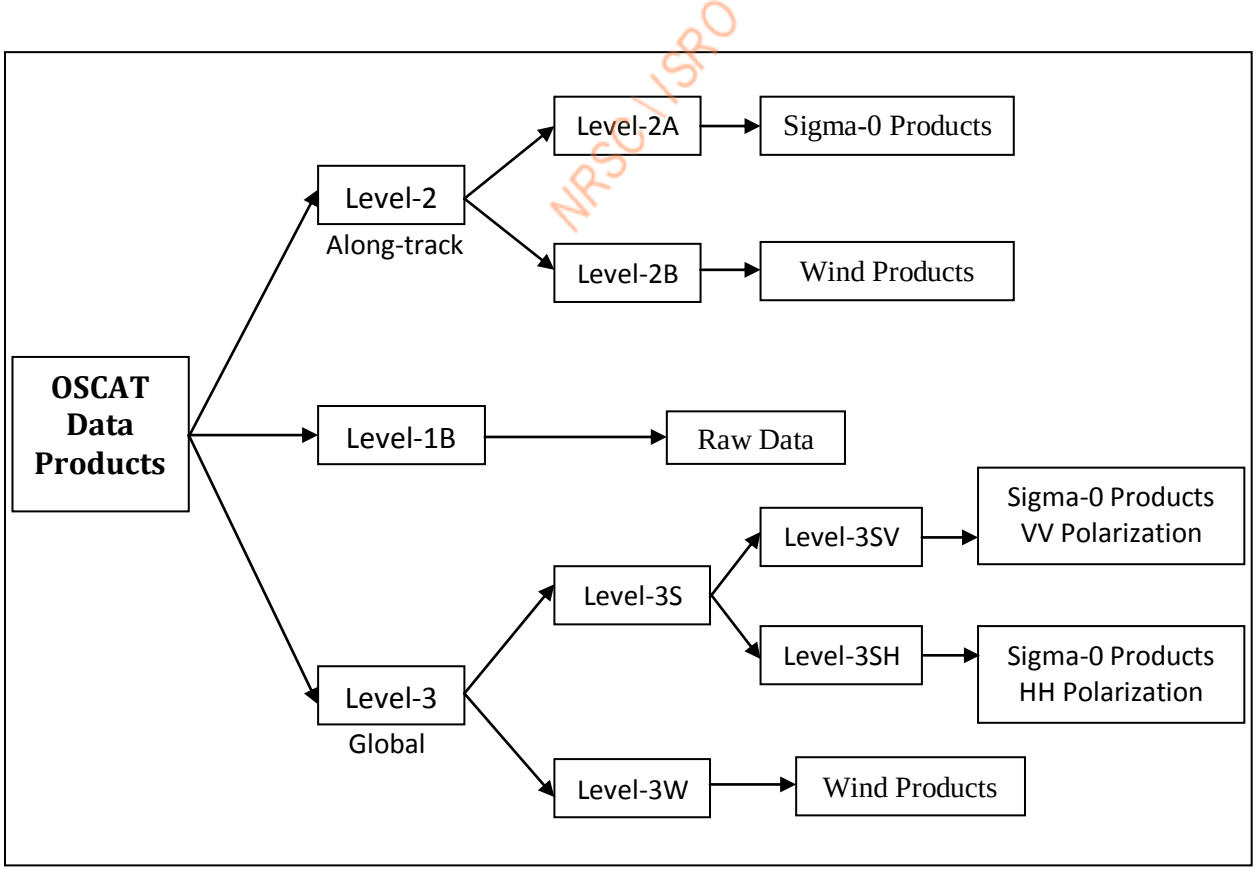

Figure 3: Details of OSCAT Data Product.

OSCAT measures the backscattered coefficient (sigma-0) which is later used to derive wind velocity vectors using Geophysical Model Functions (GMF). There are three levels of data

products available from OSCAT: Level-1B (Raw data), Level-2 (Along-track data) and Level-3 (Global gridded data). Figure 3 shows all the products obtained from OSCAT.
The OSCAT data from NRSC website is available in HDF (.h5) file format. For our computation, we have used daily composites of wind vector fields as generated using DIVA techniques on OSCAT L2B products.

The details of OSCAT data and their format can be acquired from ISRO with respective web sites of Space Application Centre (SAC) at Ahmedabad and National Remote Sensing Centre at Hyderabad and also the product handbook.

2.2 Saral/AltiKa Products

The Satellite with ARGOS and ALTIKA (SARAL) is a joint Indo-French satellite mission for oceanographic studies, which was launched on 25th February, 2013 from Satish Dhawan Space Centre, Sriharikota.

The AltiKa payload, built by French National Space Agency CNES, consists of a high-resolution single frequency altimeter (Ka-band), a dual frequency radiometer, Laser Retroreflector Array (LRA) and Doris. The 35.75 GHz AltiKa altimeter is the first oceanography altimeter to operate at such a high frequency. The foremost advantage of Ka-band is that it does not need second frequency to correct for ionospheric delay. The Ka-band altimeter also provides better vertical resolution (~ 0.3 metres) and smaller footprint (around 8 km). The dual frequency (24 and 37 GHz) radiometer allows for wet troposphere corrections in altimeter measurements.

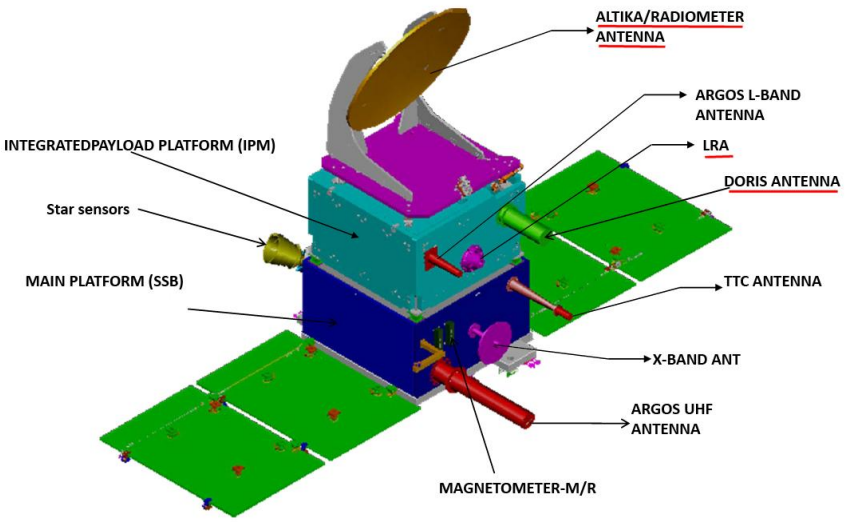

Figure 4: Saral instruments (AltiKa payload highlighted in red). (Source - AVISO)

The DORIS (Doppler Orbitography and Radiopositioning Integrated by Satellite) tracking system and LRA are used for precise measurement of orbit, location and velocity of the satellite. The details of Saral-AltiKa data products and format can be found can be acquired from respective web sites of ISRO and CNES. More information about SARAL-AltiKa and other altimeters is available on AVISO website. (http://www.aviso.oceanobs.com/)

2.3 Data-Interpolating Variational Analysis (DIVA)

DIVA is a data analysis tool developed by GeoHydrodynamic and Environmental Research (GHER) under the SeaDataNet project of the European Union [Ref. 7]. DIVA has the unique provision in-built into it to identify the coastline and topography and has a numerical coast independent of the number of observations. Automatic outlier detection based on the comparison of the data residual and the standard deviation is some of the additional features of this analysis tool. It is therefore considered suitable for the present work. Daily passes of OSCAT are merged and a daily OSCAT wind product is generated using DIVA. DIVA utilizes Variational Inverse Method (VIM) for data interpolation. Different techniques for error estimation are also in-built in DIVA software. The wind products generated using OSCAT L3 wind products are validated with an existing operational scatterometer ASCAT and also with *in situ* measured winds from RAMA and NDBP buoys in the Indian Ocean. The results are found to be encouraging [Ref. 8] and therefore, the same technique has been implemented with OSCAT L2B wind products.

2.4 Wind Stress

The horizontal force of the wind on the sea surface is called the **wind stress**, denoted by **τ.** It can also be defined as the tangential (drag) force per unit area exerted on the surface of the ocean (earth) by the adjacent layer of moving air.

To estimate surface wind stress (**τ**) for each scatterometer wind value, the following relation based on [Ref. 9] has been used:

$$\boldsymbol{\tau} = \rho C_D W^2$$

Zonal and Meridional wind stress components are computed as:

$$\tau_x = \rho_{air} C_D W^2 \sin\theta \qquad \tau_y = \rho_{air} C_D W^2 \cos\theta$$

Where,

- ρ is the density of air (1.2 kg/m^3).
- C_D is a dimensionless coefficient called **drag coefficient.**
- **W** is the wind speed.
- θ is the angle of the wind vector from true north.

Drag coefficient depends on the roughness of the surface and the lapse rate. The drag coefficient C_D for the ocean surface has a non-linear relation with the wind speed, which generally increases with wind speed.

3. Ocean Surface Currents

The Ocean surface currents are one of the dynamical features which need continuous investigation owing to their important role in various geophysical phenomena such as the transport of heat, El Nino etc. Given the large scale varying nature of currents, it is challenging to derive the current features from satellite observations. Total surface currents are primarily composed of wind driven Ekman currents and pressure gradient driven geostrophic currents.

For the computation of Ekman currents, daily composites (using DIVA) of OSCAT wind products have been used. The wind composites are available for the Indian Ocean (30^{o}S to 30^{o}N and 30^{o}E to 120^{o}E) at the spatial resolution $0.5^{o} \times 0.5^{o}$. Due to non-functioning of OSCAT in February, 2014, the total currents have been estimated for the period of March 2013 to February, 2014. Geostrophic currents have been estimated at the spatial resolution of $0.25^{o} \times 0.25^{o}$ using Sea Surface Height (SSH) data from Saral-AltiKa.

3.1 Ekman Currents

The wind-driven currents (or Ekman currents) are the resultant of frictional force exerted by wind on the ocean surface (Price et al., 1987; and Ralph and Niiler, 1999). The wind blows across the ocean and moves its waters as a result of its frictional drag on the surface. Ripples or waves cause the surface roughness necessary for the wind to couple with surface waters. Once the wind sets surface waters in motion as a current, the Coriolis Effect, Ekman transport (Figure 5), and the configuration of the ocean basin (topography) modify the speed and direction of the current. There are two-components of a wind driven current, a directly-driven Ekman component and an indirect component, due to the divergences and convergences of the Ekman transport that either leads to water piling up, creating a high pressure system in the ocean or to a low pressure system where surface waters diverge.

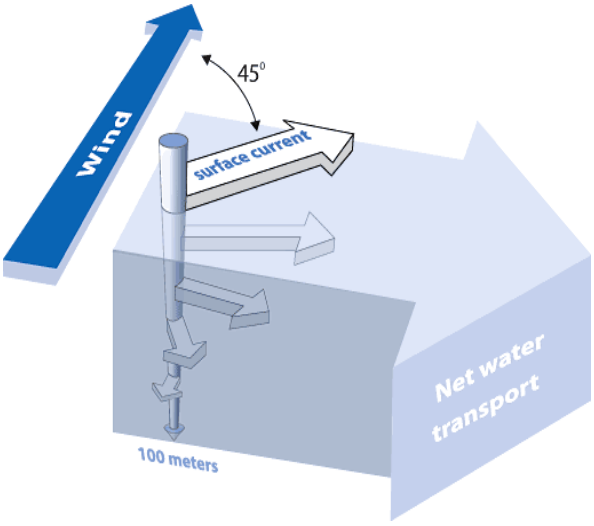

Figure 5: The Ekman motion as viewed from above in the Northern Hemisphere. The surface layer of water moves at 45° to the right of the wind. The net transport of water through the entire wind-driven column (Ekman transport) is 90° to the right of the wind.
(Source: http://oceanservice.noaa.gov/).

3.2 Geostrophic Currents

Geostrophic currents are the result of horizontal pressure gradient force and Coriolis force. Because of the Coriolis force, the current direction is perpendicular to the pressure gradient. In the *f*-plane, geostrophic currents are proportional to the height gradient divided by the Earth's rotation parameter f, which is the lowest-order balance for quasi-steady circulation at higher latitudes [*Pedlosky, 1979*]. Whereas in the *β*-plane, geostrophic balance requires special attention as f tends to 0 towards the equator. As shown in different studies, *β*-plane geostrophic approximation involving the second derivative of surface heights provides excellent agreement with the observed velocity field [*Lukas and Firing, 1984*; *Picaut et al., 1989*].

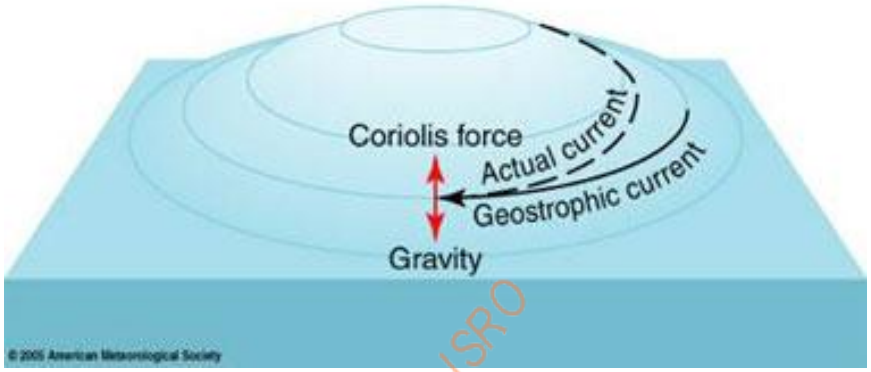

Figure 6: The geostrophic current develops when surface water while flowing downhill balance between the Coriolis force and the force arising from the horizontal water pressure gradient such that surface currents flow parallel to the contours of elevation of sea level (http://oceanmotion.org/)

3.3 Total Surface Currents

The Ekman and Geostrophic components are combined together in their respective zonal and meridional segments to obtain total currents. This provides a vector product of the ocean surface current which is represent in scatter and direction components for visualization. The data products are available as zonal and meridional components of the current. In this section, an elaborate description of data products and methodology is provided (Figure 7).

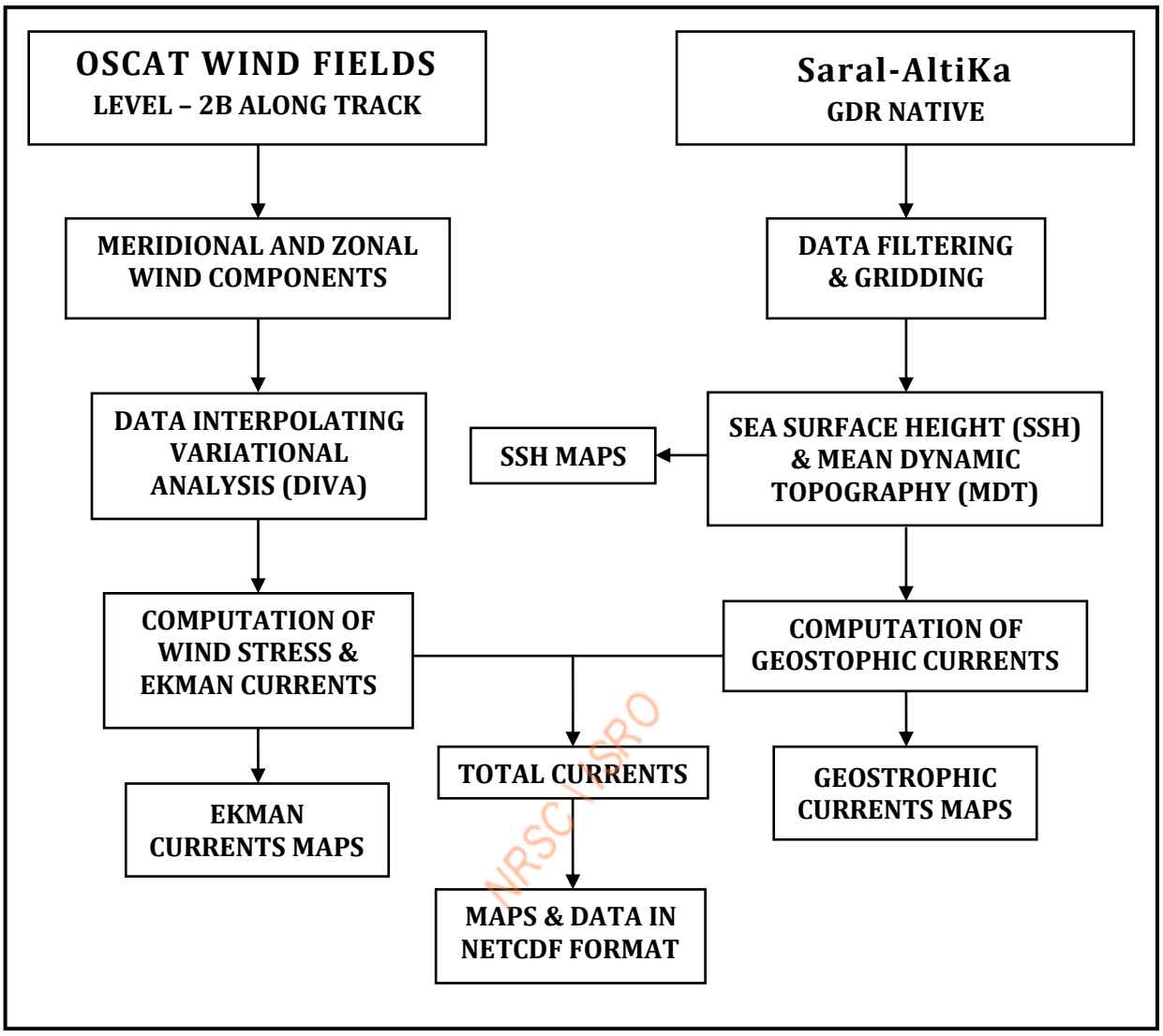

Figure 7: Flow diagram of the Currents estimation using OSCAT & Saral-AltiKa data.

The output data files are available in NETCDF (.nc) format. The images for gridded SSH, Ekman currents, Geostrophic currents and Total currents are provided in PNG image format. Gridded SSH has been computed using previous 15-days along track Saral-AltiKa OGDR and GDR products (Description is provided in next section). Figure 6 presents the flow diagram of the procedure followed for generation of daily products.

3.4 Nomenclature

Input and output file naming conventions are mentioned below:

Input file:

- OSCAT-L 2B : S1L2BYYYYDDD_NNNNN_MMMMM.h5
- AltiKa GDR : SRL_GPN_2PTPCCC_PASS_YYYYMMDD_*[1]_ YYYYMMDD_*[2].CNES.nc

Output data file:

- Total Currents : SRLP_TTT_YYYYMMDD.nc
- Geostrophic Currents : SRLP_TTT_YYYYMMDD.nc

Output images:

- Ekman Currents: OC2S_TTT_YYYYMMDD[1]_ YYYYMMDD[2].png
- Geostrophic Currents: SRLP_TTT_ YYYYMMDD[1]_ YYYYMMDD[2].png
- Sea Surface Height: SRLP_TTT_ YYYYMMDD[1]_ YYYYMMDD[2].png
- Total Currents: SRLP_TTT_ YYYYMMDD[1]_ YYYYMMDD[2].png

Where,

- YYYY : The calendar year when data was acquired.
- MM : The month when data was acquired.
- DD : The day of the month when data was acquired.
- DDD : The day of the year when data was acquired.
- YYYYMMDD[1]: Start Day (first day)
- YYYYMMDD[2]: End Day (last day)
- *[1] : Data acquisition start time (HHMMSS).
- *[2] : Data acquisition end time (HHMMSS).
- P : G → GDR
  I → IGDR
  O → OGDR
- TTT : Product Type
  TSC → Total Surface Currents
  GEO → Geostrophic Currents
  EKM → Ekman Currents
  SSH → Sea Surface Height

For more information on OSCAT-2 products, visit http://www.nrsc.gov.in/ and for Saral-AltiKa products, visit http://www.aviso.oceanobs.com/.

3.5 Data Processing Steps

The methodology for obtaining surface currents from satellites involves effectively and efficiently combining the Sea Surface Height (SSH) or Absolute Dynamic Topography (ADT) data from altimeters with the wind velocity data from scatterometers. All the current products are generated only for the Indian Ocean (30°S to 30°N and 30°E to 120°E). MATLAB tools have been used for the computation and generation of output products. The following steps have been adopted for the derivation of products:

Estimation of Ekman Currents:

For the wind-driven (Ekman) currents, the Ekman components (u_e,v_e) are given by [*Van Meurs & Niiler*, 1999]:

$$u_e + iv_e = Be^{i\varphi}(\tau_x + i\tau_y);$$
$$B = \frac{1}{\rho}(r^2 + f^2 h^2)^{-\frac{1}{2}},\ \varphi = arctan\left(\frac{fh}{r}\right) \quad \text{.....(1)}$$

Where [u_e, v_e] are the zonal and meridional ekman current components, respectively. ρ is the density of water (1025 kgm^{-3}), h is the wind mixing depth and r is a linear drag coefficient that represents vertical viscosity terms. τ_x and τ_y represent the Wind stress components, which have been directly taken from the products available at NICES portal of Bhuvan website. These stress components are computed as:

$$\tau_x = \rho_{air} C_D W^2 \sin\theta \qquad \tau_y = \rho_{air} C_D W^2 \cos\theta \quad \text{.....(2)}$$

where, C_D is a dimensionless coefficient called drag coefficient. Non-linear drag coefficient (C_D) based on Large & Pond (1981) modified for low wind speeds [Trenberth et al., 1990] is used.

W is the wind speed (taken from Daily Wind Composites products available at NICES portal), θ is the angle of wind vector from true north and ρ is the density of air (1.2 kg/m^3).
Finally it comes out to be:

$$u_e = \frac{1}{\rho(r^2 + f^2h^2)}(r\tau_x + fh\tau_y)$$
$$v_e = \frac{1}{\rho(r^2 + f^2h^2)}(r\tau_y - fh\tau_x) \quad \text{.....(3)}$$

Lagerloef et al. (1999) performed a regression analysis and found values of r = 2.15 x 10^{-4} ms^{-1} and h = 32.5 m, which remain fairly constant over the tropical band. We have used the same values in our analysis.
As the wind composite products are available at the spatial resolution of 0.5°×0.5°, for generation of Ekman currents, the products are regridded at spatial resolution of 0.25°×0.25°. The ekman currents products are available at the quarter degree resolution for the Indian Ocean.

Gridding of SSH and MDT:

SSH and MDT data has been gridded at a spatial resolution of 0.25°×0.25° for the complete global. For gridding, Saral-AltiKa GDR native data set for the last 15 days has been filtered

and then, accumulated for each 0.25° grid cell and the median value is allotted to that particular grid cell. SSH is defined at the sum of Sea Surface Height Anomaly (SSHA) and MDT. For accumulation, all the observations lying within a latitudinal separation of 0.125 degrees and longitudinal separation of 0.5 degrees from each grid cell are taken.

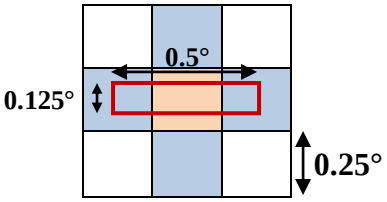

The filtering of the data has been carried out as per the conditions provided by the document available at AVISO website:

1	surface_type	0
2	ice_flag	0
3	rad_surf_type	0
4	range_numval	20 ≤ x
5	range_rms	0 ≤ x (mm) ≤ 200
6	altitude – range	-130 000 ≤ x (mm) ≤ 100 000
7	model_dry_tropo_corr	-2 500 ≤ x (mm) ≤ -1900
8	rad_wet_tropo_corr	-500 ≤ x (mm) ≤ -20
9	iono_corr_alt	-100 ≤ x (mm) ≤ 40
10	sea_state_bias	-500 ≤ x (mm) ≤ 0
11	ocean_tide_sol1	-5 000 ≤ x (mm) ≤ 5 000
12	solid_earth_tide	-1 000 ≤ x (mm) ≤ 1000
13	pole_tide	-150 ≤ x (mm) ≤ 150
14	swh	0 ≤ x (mm) ≤ 11 000
15	sig0	3 ≤ x (dB) ≤ 30
16	off_nadir_angle_wf	-0.2 ≤ x (deg^2) ≤ 0.64
17	sig0_rms	x (dB) ≤ 1
18	sig0_numval	20 < x
19	ssha + mean_topography	0 < x

Table 1: Satal-AltiKa flags for the selection of best data (Source: AVISO)

After applying all the above mentioned filters and flags, median of all the observations (from last 15 days) lying within 0.25° of each grid cell is allotted to that particular cell. This gridded SSH and MDT is further smoothed using moving average technique with the window of 1.25° x 1.25° (i.e. 5 x 5 grid cells).

Estimation of Geostrophic Currents:

From this absolute dynamic topography, the geostrophic currents are then to be computed as the gradient of ADT. In the f-plane, the two components i.e. east and north ($u_{g,f}$, $v_{g,f}$) of the surface geostrophic current vector are then given as:

$$u_{g,f} = -\frac{g}{f}\frac{\partial \zeta}{\partial y}, \qquad V_{g,f} = \frac{g}{f}\frac{\partial \zeta}{\partial x} \quad \text{.....(4)}$$

where, g is the acceleration due to gravity, f is the Coriolis parameter ($f = 2\,\Omega \sin \varphi$), and ζ is the height of the sea surface above a level surface (ADT). φ is the latitude and Ω is the angular velocity of the earth's rotation ($\Omega = 7.29 \times 10^{-5}$ sec^{-1}).
In the β-plane, as shown by Lagerloef at al. (1999) the geostrophic currents ($u_{g,\beta}$, $v_{g,\beta}$) are computed as:

$$u_{g,\beta} = -\frac{g}{\beta}\frac{\partial^2 \zeta}{\partial^2 y}, \quad V_{g,\beta} = \frac{g}{\beta}\frac{\partial^2 \zeta}{\partial x \partial y} \quad \text{.....(5)}$$

where, $\beta = \frac{\partial f}{\partial y}$.

For the equatorial region, β is a constant given by $\beta = 2\,\Omega/r = 2.3 \times 10^{-11}$ m^{-1}s^{-1}. Picaut et al. (1989) also state that the second derivative is valid over spatial scales of > 100 km and timescales greater than 15-30 days, providing relatively smoothed geostrophic velocities at the equator. The computation of Geostrophic currents in the Indian equatorial region requires further investigation.

The final currents are then a linear combination of geostrophic and wind-driven (Ekman) motion given as:

$$\bar{U} = \bar{U}_g + \bar{U}_e \quad \text{.....(6)}$$

where, $\bar{U}_g$ *and* $\bar{U}_e$ are the Geostrophic and Ekman components, respectively.

4. Results and Discussion

The Saral-AltiKa and OSCAT derived ocean surface currents have been compared with CNES AVISO geostrophic currents and NOAA OSCAR total currents for the year 2013 (i.e. 28th Mar, 2013 to 31st Dec, 2013). Both the AVISO and OSCAR currents data are available at spatial resolution of 0.33° with temporal resolution of daily and 5 days respectively. The datasets are regridded to the spatial resolution of 0.25° using nearest neighborhood method. The results have been indicated. The validation of the currents is still in progress, but the preliminary results are very promising. The comparisons are also carried out at different spatial and temporal resolutions.

4.1 Comparison with AVISO Geostrophic currents

The comparison results of Saral-AltiKa derived geostrophic currents with AVISO geostrophic currents are shown in Tables 2 & 3. As can be seen, geostrophic currents in f-plane show better correlation than those in β-plane. This can be attributed to Coriolis parameter which

approaches zero in the β-plane. Also, the zonal component of geostrophic currents shows better correlation than meridional component. The bias in currents speed (f-plane) varies in the range of 3.5 – 4.5 cm/s. The correlation is highest for the months of August and September. As the products are still in testing phase, it will be difficult to comment on the causes of these discrepancies.

Month	R_U	R_V	R_W	Bias_U	Bias_V	Bias_W
Mar	0.46	0.32	0.35	-0.01	0.83	3.50
Apr	0.51	0.31	0.42	-0.32	0.77	4.07
May	0.55	0.33	0.45	0.32	0.90	4.35
Jun	0.53	0.36	0.44	0.57	0.86	4.68
Jul	0.56	0.37	0.46	0.08	1.07	4.41
Aug	0.60	0.40	0.49	-0.33	0.79	3.45
Sep	0.60	0.40	0.49	-0.46	0.71	3.56
Oct	0.57	0.40	0.43	-0.15	0.69	3.82
Nov	0.54	0.40	0.37	0.59	0.67	4.37
Dec	0.54	0.37	0.42	0.25	0.39	4.26

Table 2: AVISO versus Saral-AltiKa derived geostrophic currents for 2013. Monthly mean values of correlation coefficient (R) and bias (in cm/s) have been indicated for zonal(U), meridional (V) and total (W) currents.

Month	R_U	R_V	R_W	Bias_U	Bias_V	Bias_W
Mar	0.66	0.46	0.50	0.79	0.28	-1.25
Apr	0.65	0.45	0.50	0.66	0.20	0.02
May	0.66	0.44	0.51	0.40	0.15	0.04
Jun	0.66	0.48	0.55	0.50	0.34	0.15
Jul	0.72	0.53	0.61	0.17	0.42	-0.60
Aug	0.74	0.53	0.63	0.30	0.21	-0.92
Sep	0.74	0.53	0.64	0.10	0.29	-0.87
Oct	0.72	0.53	0.58	0.18	0.31	-0.82
Nov	0.71	0.55	0.54	0.38	0.21	-1.05
Dec	0.69	0.51	0.55	0.38	0.24	-0.85

Table 3: AVISO versus Saral-AltiKa derived geostrophic currents in the f-plane (|latitude| > 5) for 2013. Monthly mean values of correlation coefficient (R) and bias (in cm/s) have been indicated for zonal (U), meridional (V) and total (W) currents.

4.2 Comparison with OSCAR total currents

The comparison results of Saral-AltiKa and OSCAT derived total currents with OSCAR geostrophic currents are shown in Table 4 & 5. As was observed in the case of AVISO, currents in f-plane show better correlation than those in β-plane. Also, the zonal component of currents shows better correlation than meridional component. The bias in currents speed (f-plane) has now reduced to the range of 1 – 3 cm/s. In this case also, the correlation is highest for the months of August and September.

Month	R_U	R_V	R_W	Bias_U	Bias_V	Bias_W
Mar	0.49	0.41	0.55	2.31	0.10	0.13
Apr	0.52	0.32	0.55	-0.23	0.40	1.58
May	0.62	0.34	0.60	-0.29	0.39	1.12
Jun	0.57	0.35	0.57	1.93	-0.63	3.84
Jul	0.54	0.37	0.56	1.20	0.60	3.03
Aug	0.60	0.40	0.60	0.46	0.43	2.64
Sep	0.67	0.47	0.61	-0.57	0.05	2.55
Oct	0.62	0.47	0.58	0.92	0.20	2.59
Nov	0.59	0.46	0.56	0.61	0.37	2.90
Dec	0.67	0.42	0.62	-0.66	-0.67	2.69

Table 4: OSCAR versus Saral-AltiKa derived total currents for 2013. Monthly mean values of correlation coefficient (R) and bias (in cm/s) have been indicated for zonal(U), meridional (V) and total (W) currents.

Month	R_U	R_V	R_W	Bias_U	Bias_V	Bias_W
Mar	0.72	0.54	0.54	0.26	-0.71	-0.51
Apr	0.70	0.49	0.54	1.04	0.26	0.91
May	0.72	0.47	0.55	0.57	-0.65	1.05
Jun	0.77	0.51	0.58	1.01	-2.13	2.87
Jul	0.78	0.53	0.64	0.59	-1.36	1.64
Aug	0.81	0.57	0.68	0.46	-1.32	1.64
Sep	0.83	0.61	0.70	0.11	-0.88	1.46
Oct	0.80	0.60	0.64	0.35	-0.27	1.02
Nov	0.78	0.62	0.59	0.24	0.43	0.84
Dec	0.77	0.58	0.60	-0.09	0.42	1.35

Table 5: OSCAR versus Saral-AltiKa derived total currents in the f-plane (|latitude| > 5) for 2013. Monthly mean values of correlation coefficient (R) and bias (in cm/s) have been indicated for zonal (U), meridional (V) and total (W) currents.

4.3 Comparison with moored buoy total currents

The currents from satellite and INCOIS moored buoys have been compared and the results are indicated in figure 8 & 9. The comparisons have been carried out at different spatial and temporal resolutions. A preliminary analysis indicated that the satellites derived currents exhibit better correlation in Bay of Bengal region rather than Arabian Sea region. This may be attributed to general feature of low surface currents in Arabian Sea. It has also been observed that comparison at 50 km spatial resolution shows better results.

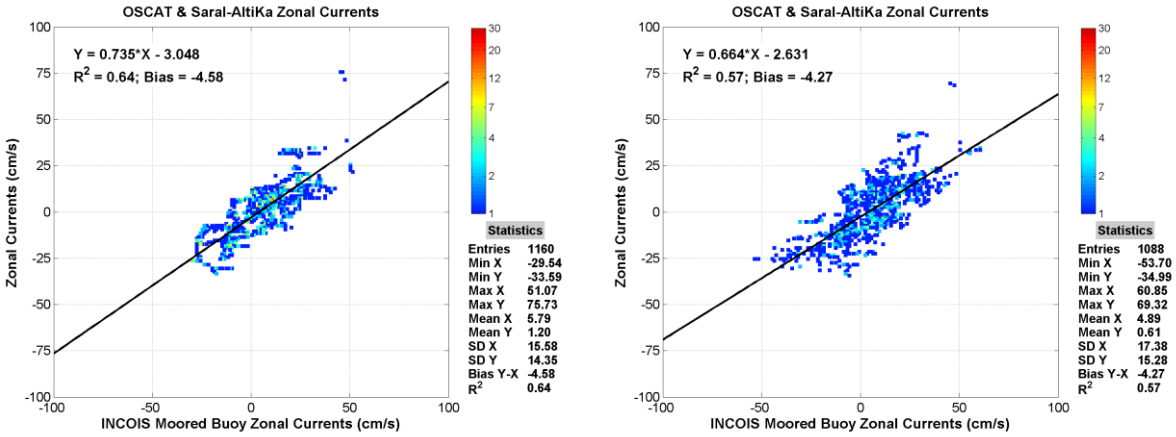

Figure 8: (Left) Comparison of OSCAT and Saral-AltiKa derived ocean surface zonal currents with INCOIS moored buoy ocean zonal currents at 25 km spatial resolution on monthly basis for Bay of Bengal region. (Right) Comparison of OSCAT and Saral-AltiKa derived ocean surface zonal currents with INCOIS moored buoy ocean zonal currents at 100 km spatial resolution on weekly basis for Bay of Bengal region.

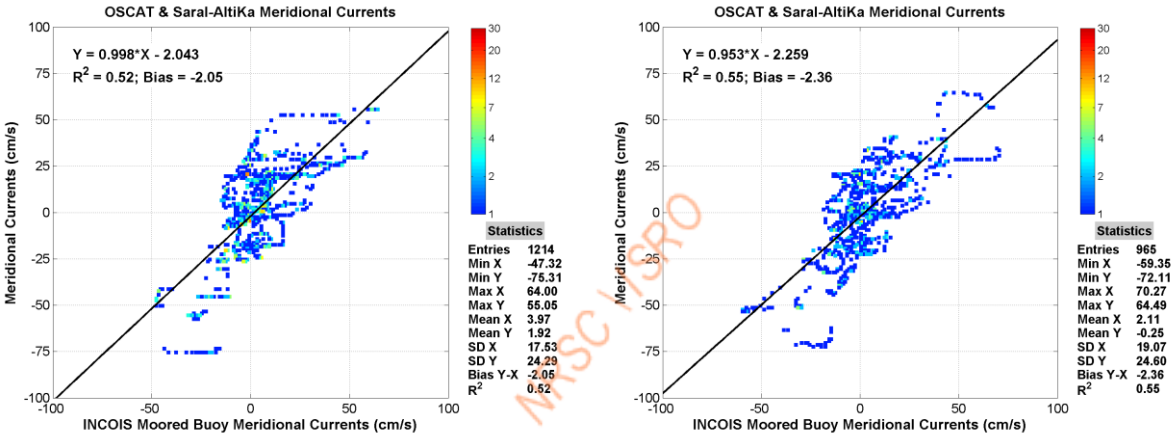

Figure 9: (Left) Comparison of OSCAT and Saral-AltiKa derived ocean surface meridional currents with INCOIS moored buoy ocean meridional currents at 25 km spatial resolution on monthly basis for Bay of Bengal region. (Right) Comparison of OSCAT and Saral-AltiKa derived ocean surface meridional currents with INCOIS moored buoy ocean meridional currents at 50 km spatial resolution on 15 days mean basis for Bay of Bengal region.

Please note that INCOIS moored buoys measure ocean currents at 3 metres depth.

Further improvement in algorithm can be expected in upcoming versions of the same document.

As Saral-AltiKa derived geostrophic currents can be estimated using OGDR data, the products are generated on real time basis. The processing is done in real time, with geostrophic currents already estimated from 28th March, 2013 onwards on daily basis. But as OSCAT data is only available till February, 2014, the total surface currents are available for the period of March, 2013 to February, 2014. For an example, map of Saral-AltiKa derived geostrophic currents is shown in figure 10. As can be observed from the figure, major gyre systems and general circulation pattern in the Indian Ocean region can be easily distinguished. The Somalia region gyre is further discussed in next figure.

As shown in figure 10, the net geostrophic currents flow in the western equatorial region is eastward, whereas in the northern part of eastern equatorial region, it is eastward. Also, the major gyre systems are prominently evident in the currents maps.

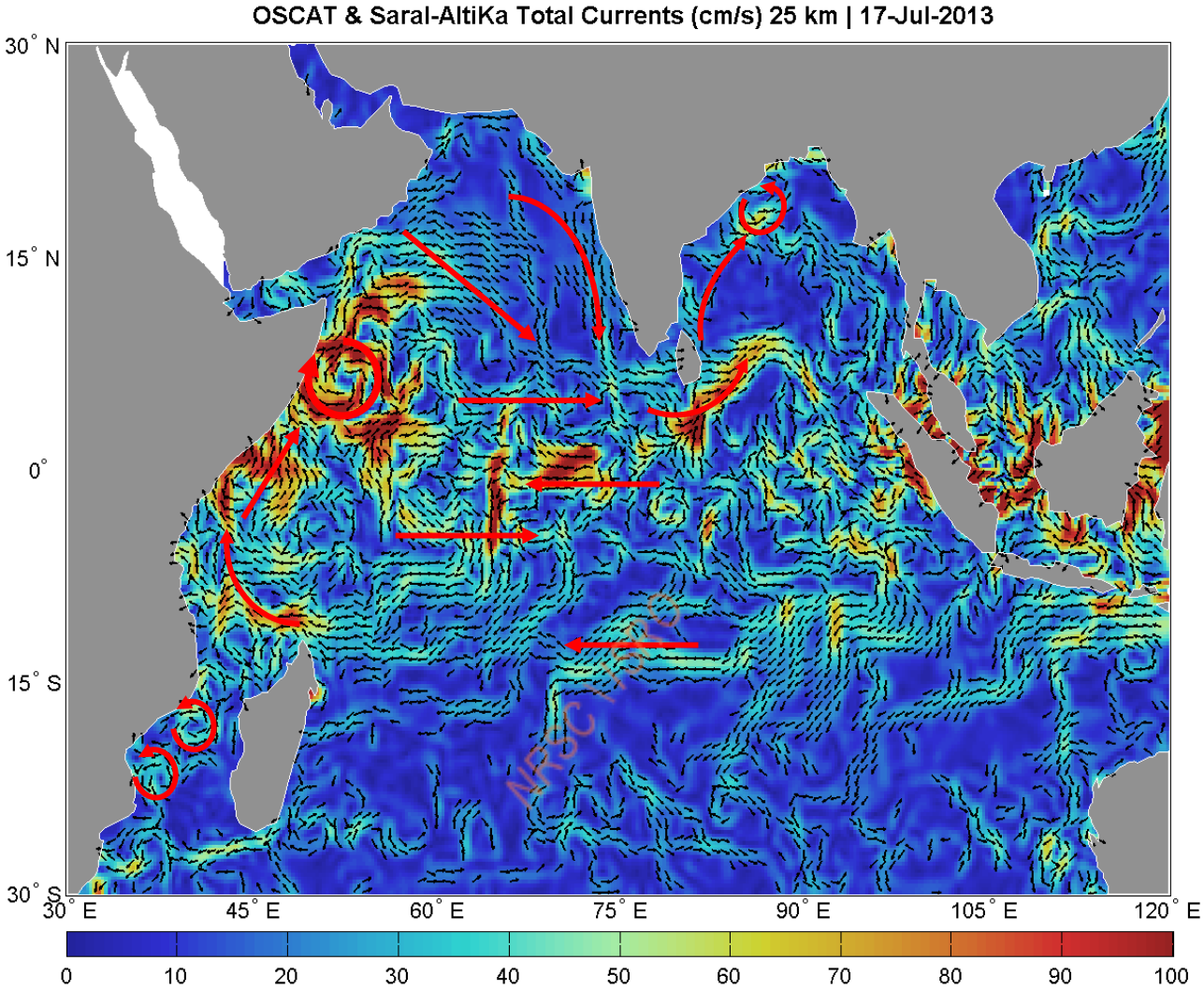

Figure 10: Saral-AltiKa derived Geostrophic currents for 04 June, 2014. The red arrows indicate the gyre systems and the general flow pattern.

Similar Indian Ocean total surface maps have been generated on daily basis. In the next figure, high resolution images of total ocean surface currents are shown for Somali and Bay of Bengal region.

Figure 11 shows Somali current system, which varies significantly with time. (Left) During summer (June) i.e. southwest monsoon, the Somali currents flow towards north-east giving rise to upwelling along the coast of Somalia. (Right) With the onset of winter (Jan) monsoon, the Somali currents completely reverse their direction and flow towards southwest along the Somalia coast, and thereby, no upwelling.

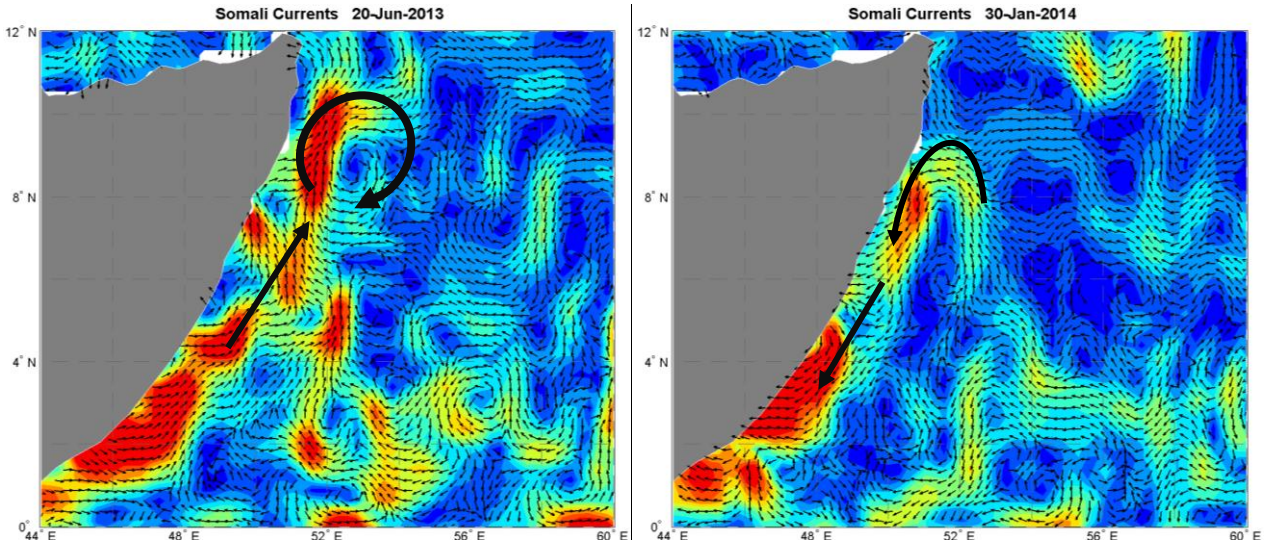

Figure 11: Somalia region total surface currents for 20 June, 2013 (Left) and 30 January, 2014 (Right). The red arrows indicate the gyre systems and the general flow pattern. Scale same as Figure 3.

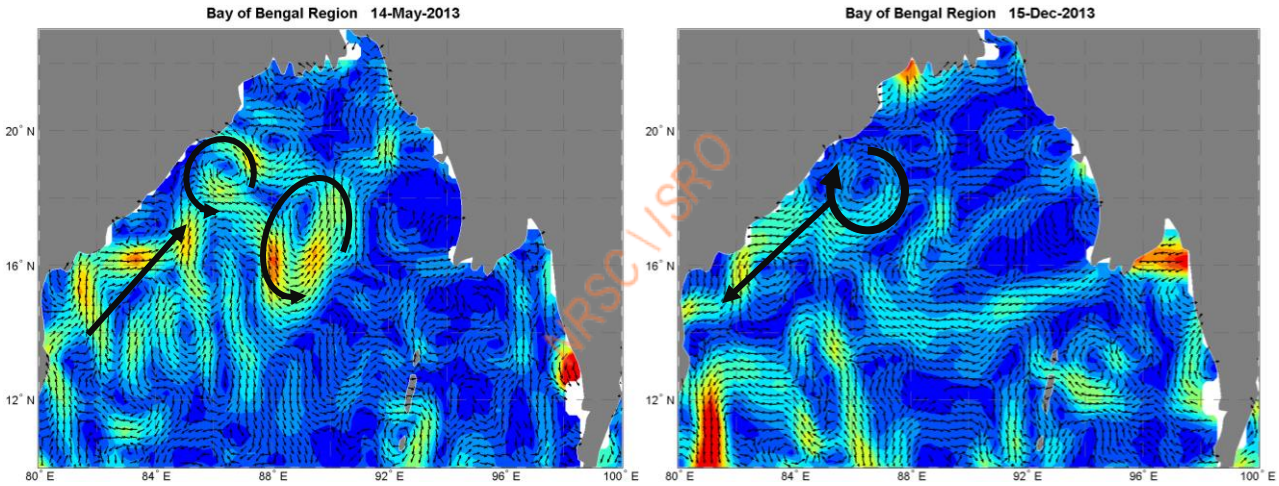

Figure 12: Bay of Bengal region total surface currents for 14 May, 2013 (Left) and 15 December, 2013 (Right). The red arrows indicate the gyre systems and the general flow pattern. Scale same as Figure 3.

Figure 12 shows effects of monsoon on the ocean surface currents along the eastern coast of India in Bay of Bengal. (Left) During summer (May) i.e. with the onset of southwest monsoon, the currents along the east coast of India flow towards north-east giving rise to upwelling along the coast. (Right) With the onset of winter (Dec) monsoon, the currents completely reverse their direction and flow towards southwest.

5. Conclusion

The ocean surface currents derived using products of OSCAT and Saral-AltiKa show very promising results. The salient features of Indian Ocean circulation, with seasonal variations are reflected in the total surface currents. As can be observed from the figure 9, major gyre

systems and general circulation pattern in the Indian Ocean region can be easily distinguished. The Somalia region gyre is further discussed in next figure. Also, the preliminary validation results at different spatial and temporal resolutions with INCOIS buoys show promising correlation coefficient (R^2) ranging from 0.52 to 0.64. Bias for zonal currents is more negative (≈ −4 cm/s) than that for meridional component (≈ −2 cm/s). There is a scope for better results by performing global validation and fine tuning of algorithm. Better results can be expected in the upcoming versions of total surface currents.

Acknowledgements: We take it as a deemed privelege to express our sincere thanks to all concerned who have contributed either directly or indirectly for the successful completion of ocean surface currents computation and product generation using Saral-AltiKa altimeter and Oceansat-2 scatterometer data.
The work is a part of Techincal Development Project (TDP) at NRSC and SARAL-AltiKa User Promotion activity of ISRO. We are highly grateful to Dr. V. K. Dadhwal, Director NRSC for his encouragement and guidance during this study. NDC team and network support group of NRSC and last but not the least OSCAT project team are sincerely acknowledged for successfully making OSCAT data available to the users.

6. References

AVISO User Handbook Ssalto/Duacs: M(SLA) and M(ADT) Near-Real Time and Delayed-Time, *SALP-MU-P-EA-21065-CLS*, edition 4.1, May 2014 (AVISO - Archiving, Validation and Interpretation of Satellite Oceanographic Data) www.oceanobs.aviso.com

Bonjean, F. and Gary S. E. Lagerloef (2002), Diagnostic model and analysis of the surface currents in the tropical Pacific ocean, *J. Phys. Oceanogr.*, 32, 29382954.

Dorandeu, J. and P. Y. Le Traon (1999), Effects of global mean atmospheric pressure variations on mean sea level changes from TOPEX/Poseidon, *J. Atmos. Oceanic Technol.*, 16, 1279–1283.

Ducet, N., P. Y. Le Traon and G. Reverdin (2000), Global high resolution mapping of ocean circulation from TOPEX/Poseidon and ERS 1 and 2, *J. Geophys. Res.*, 105 (C8), 19,477-19,498.

Lagerloef, G. S. E., G. T. Mitchum, R. Lukas and P. P. Niiler (1999), Tropical pacific near surface currents estimated from altimeter, wind and drifter data, *J. Geophys. Res.*, 104, 23,313–23,326.

Le Traon, P.-Y. and F. Ogor(1998), ERS-1/2 orbit improvement using TOPEX/Poseidon: The 2 cm challenge, *J. Geophys. Res.*, 103, 8045–8057.

Lukas, R. and E. Firing, 1984: The geostrophic balance of the Pacific Equatorial Undercurrent, Deep-Sea Res., 31, 61–66.

OSCAT Product Handbook, Version 1.3, Dec. 2011.

Price, J. F., R. A. Weller and R. R. Schudlich (1987), Wind-Driven Ocean Currents and Ekman Transport, *Science*, 238 (4833), 1534-1538.

Geophysical fluid dynamics, Joseph Pedlosky. Springer-Verlag, Berlin,1979

Philander, S. G. H. and R. C. Pacanowski (1980), The generation of equatorial currents, *J. Geophys. Res.*, 85, 1,123–1,136.

Picaut J, Hayes SP, McPhaden MJ (1989) Use of the geostrophic approximation to estimate time-varying zonal currents at the equator. J Geophys Res 94:3228–3236.

Ralph, E. A. and P. P. Niiler (1999), Wind-driven currents in the tropical pacific, *J. Phys. Oceanogr.*, 29, 2121–2129.

Saral-AltiKa Products Handbook, *SALP-MU-M-OP-15984-CN*, Issue 2.3, July 2013.

Seidel HF, Giese BS (1999) Equatorial currents in the Pacific Ocean 1992–1997. J Geophys Res 104:7849–7863

Stommel, H. (1960), Wind-drift near the equator, *Deep Sea Res.*, 6, 298–302.

Sudre,J. and R. Morrow (2008), Global surface currents: a high-resolution product for investigating ocean dynamics, *Ocean Dynamics*, DOI 10.1007/s10236-008-0134-9.

K.E. Trenberth, W.G. Large & J.G. Olson, 1990, "The Mean Annual Cycle in Global Ocean Wind Stress", *J.Physical Oceanography*, Vol. 20, pp. 1742 – 1760.

Van Meurs P, Niiler PP (1997), Temporal variability of the large-scale geostrophic surface velocity in the northeast Pacific, *J. Phys. Oceanogr.*, 27:2288–2297

W. G. Large & S. Pond., 1981,"Open Ocean Measurements in Moderate to Strong Winds", *J. Physical Oceanography*, Vol. 11, pp. 324 - 336.

7. Appendix

Ouptut Netcdf file structure

```
Global attributes:
  :Title = "Daily Surface Currents using OSCAT & Saral-AltiKa";
  :Version = "1.0";
  :Organization_Name = "ISRO-DOS";
  :Processing_Centre = "NRSC";
  :Satellite_Name_1 = "Oceansat-2";
  :Intrument_1 = "OSCAT - Scatterometer";
  :Satellite_Name_2 = "Saral-AltiKa";
  :Intrument_2 = "AltiKa - Altimeter";
  :Resolution = "0.25 x 0.25 degress";
  :Product_Date = "DD-MMM-YYYY";
  :Conventions = "CF-1.6";
  :Creation_Date = "YYYY/MM/DD hh:mm:ss";
  :Created_By = "OSG/ECSA";
  :Comment = "Check the technical documents for more information.";
  :_CoordSysBuilder = "ucar.nc2.dataset.conv.CF1Convention";

Dimensions:
    latitude = 240;
    longitude = 360;
    day = 1;

Variables:
  double mdt(day=1, longitude=360, latitude=240);
      :standard_name = "mean dynamic topography";
      :long_name = "mean dynamic topography";
      :units = "cm";
      :comment = "mean topography";

    double ssh(day=1, longitude=360, latitude=240);
      :standard_name = "sea surface height";
      :long_name = "sea surface height";
      :units = "cm";
      :comment = "sum of mean topography and sea surface anomaly";

    double u_ekm(day=1, longitude=360, latitude=240);
      :standard_name = "zonal ekman currents";
```

```
      :long_name = "zonal ekman currents";
      :units = "cm/s";
      :comment = "Wast-east component of Ekman Currents";

    double v_ekm(day=1, longitude=360, latitude=240);
      :standard_name = "meridional ekman currents";
      :long_name = "meridional ekman currents";
      :units = "cm/s";
      :comment = "South-north component of Ekman Currents";

    double u_geo(day=1, longitude=360, latitude=240);
      :standard_name = "zonal geostrophic currents";
      :long_name = "zonal geostrophic currents";
      :units = "cm/s";
      :comment = "Wast-east component of Geostrophic Currents";

    double v_geo(day=1, longitude=360, latitude=240);
      :standard_name = "meridional geostrophic currents";
      :long_name = "meridional geostrophic currents";
      :units = "cm/s";
      :comment = "South-north component of Geostrophic Currents";

    double u_total(day=1, longitude=360, latitude=240);
      :standard_name = "zonal surface currents";
      :long_name = "zonal total ocean surface currents";
      :units = "cm/s";
      :comment = "Computed by adding zonal components of Ekman &
Geostrophic Currents.";

    double v_total(day=1, longitude=360, latitude=240);
      :standard_name = "meridional surface currents";
      :long_name = "meridional total ocean surface currents";
      :units = "cm/s";
      :comment = "Computed by adding meridional components of Ekman &
Geostrophic Currents.";

    double latitude(latitude=240);
      :standard_name = "latitude";
      :long_name = "latitude";
      :units = "degrees_north";
      :limits = "-30N to 30N in degrees";
      :comment = "Positive latitude is North latitude, negative latitude is
South latitude.";
      :_CoordinateAxisType = "Lat";

    double longitude(longitude=360);
      :standard_name = "longitude";
      :long_name = "longitude";
      :units = "degrees_east";
      :limits = "30E to 120E in degrees";
      :comment = "East longitude relative to Greenwich meridian.";
      :_CoordinateAxisType = "Lon";

    int day(day=1);
      :standard_name = "day";
      :long_name = "day number";
      :units = "days since 2000-1-0";
      :comment = "Day number since 1-Jan-2000. 1-Jan-2000 is Day number
1.";
      :_FillValue = -99999; // int
```

Ocean Sciences Group
(Earth and Climate Science Area)
National Remote Sensing Centre
ISRO (Govt. of India, Dept. of Space)
Balanagar, Hyderabad – 500037, INDIA

NRSC – ECSA – OSG – NOV - 2014 – TR – 659